IEEE Access
Multidisciplinary | Rapid Review | Open Access Journal

Received 2 May 2023, accepted 16 May 2023, date of publication 22 May 2023, date of current version 1 June 2023.

Digital Object Identifier 10.1109/ACCESS.2023.3278278

RESEARCH ARTICLE

Automated Detection of Diabetes From Exhaled Human Breath Using Deep Hybrid Architecture

NAVANEETH BHASKAR[1], VINAYAK BAIRAGI[2], (Senior Member, IEEE), EKKARAT BOONCHIENG[3], (Senior Member, IEEE), AND MOUSAMI V. MUNOT[4]

[1]Faculty of Computer Science and Engineering (Data Science), Sahyadri College of Engineering and Management, Mangaluru 575007, India
[2]Department of Electronics and Telecommunication Engineering, AISSMS Institute of Information Technology, Pune 411001, India
[3]Center of Excellence in Community Health Informatics, Faculty of Science, Chiang Mai University, Chiang Mai 50200, Thailand
[4]Department of Electronics and Telecommunication Engineering, Pune Institute of Computer Technology, Pune 411043, India

Corresponding author: Ekkarat Boonchieng (ekkarat@ieee.org)

This work was supported in part by the Chiang Mai University and National Science, Research and Innovation Fund (NSRF) via the Program Management Unit for Human Resources and Institutional Development, Research and Innovation under Grant B05F640183.

This work involved human subjects or animals in its research. Approval of all ethical and experimental procedures and protocols was granted by the Institutional Research Ethics Review and Use Committee (IRERUC) and performed in line with the Declaration of Helsinki.

ABSTRACT In this paper, we have proposed an automated medical system for detecting type 2 diabetes from exhaled breath. Human breath can be used as a diagnostic sample for detecting many diseases as it contains many gases that are dissolved in the blood. Breath-based analysis stands out among the different non-invasive ways of detection as it provides more accurate predictions and offers many advantages. In this work, the concentration of acetone in the exhaled breath is analysed to detect type 2 diabetes. A new sensing module consisting of an array of sensors is implemented for monitoring the acetone concentration to detect the disease. Deep learning algorithms like Convolutional Neural Networks (CNN) are normally used to automatically analyse medical data to make predictions. Even though the CNN performs well, a few modifications to the network layout can further improve the classification accuracy of the learning model. To analyse the sensor signals to generate predictions, a new deep hybrid Correlational Neural Network (CORNN) is designed and implemented in this research. The proposed detection approach and deep learning algorithm offer improved accuracy when compared to other non-invasive techniques.

INDEX TERMS Acetone, breath, convolutional neural network, correlation, deep learning, diabetes, neural network.

I. INTRODUCTION

Diabetes is a chronic disease that requires frequent blood glucose testing. The World Health Organization's most recent statistics indicate that there are more than 500 million diabetic patients worldwide, and around 1.6 million people die each year due to diabetes and related disorders. The number of people living with diabetes may reach 780 million by 2045, according to reports from the International Diabetes Federation (IDF). To prevent or delay long-term health issues associated with diabetes, it is necessary to keep the sugar levels at the desired level. The hormone insulin, which is created in the pancreas, regulates the body's blood glucose level [1]. When blood glucose levels rise, the insulin production increases in the pancreas to counteract the rise. This helps maintain the blood glucose level within the normal range in a healthy person. In type 2 diabetic patients, the body cannot produce enough insulin to adequately counteract the rise in blood glucose levels. Monitoring the level of glucose in a blood sample is the clinically accepted way for detecting diabetes [2]. There is an increasing need for a non-invasive technique of monitoring diabetes because traditional diabetes detection is an invasive process.

According to medical studies, small amounts of glucose are found in saliva, tears, sweat and urine [3]. These biological samples offer the potential for non-invasive glucose level

The associate editor coordinating the review of this manuscript and approving it for publication was Gyorgy Eigner.

TABLE 1. Biomarkers identified in exhaled breath to detect various diseases.

Biomarker	Disease	Reference
Acetone	Diabetes	[7]
Nitric oxide	Asthma	[8]
Ammonia	Kidney disease	[9]
Pentane	Myocardial infarction	[10]
Methane	Cancer	[11]
Hydrogen cyanide	Cystic fibrosis	[12]

prediction in the body. Recent research has shown that the analysis of breath is a reliable non-invasive method to check glucose levels in the body [4], [5]. The primary components of the exhaled breath are oxygen (13%–16%), nitrogen (78%-79%), carbon dioxide (4%-6%) and approximately 2% of other gases including Volatile Organic Compounds (VOCs). More than 300 VOCs, which are rich in physiological and metabolic information, are excreted by a human during respiration. Certain biomarkers are found in the breath, and tracking their levels reveals the potential presence of numerous chronic conditions [6]. Table 1 provides a list of some of the biomarkers that have already been identified in exhaled breath to detect various diseases.

Acetone, a volatile chemical compound exhaled during breathing, is closely related to the body's blood sugar levels. Therefore, diabetes can be identified by monitoring the acetone levels in human breath. According to medical research, the amount of acetone in the breath of a healthy person and a diabetic patient will differ. In healthy individuals, acetone levels are normally less than 0.9 parts per million (ppm), but they are greater than 1.7 ppm in diabetic patients [13]. There are many sensors available to measure the concentrations of acetone gas. However, there is no specific sensing module available for measuring the acetone level in the exhaled breath. Due to the inadequacy of the traditional acetone detection methods for automated detection, a new detection module is created and deployed in this study. The amount of acetone in the breath is measured using a Metal Oxide Semiconductor (MOS) based gas sensor. As the acetone estimation is impacted by various parameters like humidity, temperature and pressure values in the detection chamber, we have used an array of sensors in the detection part.

In order to identify diseases and make automated predictions, machine learning techniques are commonly employed in biomedical signal processing applications [14]. The classification task in machine learning is carried out by using various machine learning algorithms. The main advantage of using machine learning networks is that, after learning, these algorithms can automatically perform the assigned goal. With these techniques, we can teach the machines to analyze data more quickly and efficiently. Machine learning offers a variety of feature extraction and classification algorithms. For feature extraction and classification, two different algorithms are often used in traditional machine learning methods. Recent studies have employed Convolutional Neural Network (CNN) models in place of traditional machine learning methods for making the prediction [15]. The CNN itself performs both feature extraction and classification tasks in CNN learning networks. As a result, CNN networks do not need a separate feature extraction module. Compared to traditional machine learning networks, CNN delivers more accurate outcomes when addressing real-time problems. In this study, a new deep learning Correlational Neural Network (CORNN) model that gives greater classification accuracy is developed and employed for the classification of the samples. The proposed network, as its name suggests, extracts the features from the sample using a correlation layer rather than a convolution layer. With the proposed medical system, anyone can be assisted in making a clinical decision without the assistance of doctors.

II. ARCHITECTURE OF THE CORRELATIONAL NEURAL NETWORK

The proposed CORNN architecture is designed by amending the architecture of conventional CNN. To get the best features out of the sensor response signal, we used the correlation operation rather than the convolution. Fig. 1 depicts the conceptual layout of the CORNN learning model. The network has layers of correlation and sub-sampling, followed by a layer for classification. The key component of this model is the correlational part. The procedure of feature extraction is used to extract the important features from the input signal.

In signal-processing applications, convolution and correlation techniques are extensively utilised. The fundamental correlation operation involves applying the filter to the input signal and computing the sum of the products of the overlapping data [16]. By using the same filter on the whole input signal, this procedure is repeated. The following equation represents the correlation procedure between the two signals:

$$k_r \circ I(x) = \sum_{i=-N}^{N} k_r(i) I(x+i) \tag{1}$$

where I represent the input signal and k_r represents the kernel.

Similarly, for a 2-D signal, the equation is represented as:

$$k_r \circ I(x,y) = \sum_{j=-N}^{N} \sum_{i=-N}^{N} k_r(i,j) I(x+i, y+j) \tag{2}$$

A minor distinction separates the convolution from the correlation procedure. Before executing the signal convolution procedure, the filter is rotated 180 degrees in the convolution operation. The mathematical representation of the convolution procedure for 1-D and 2-D input signals is as follows:

$$k_r * I(x) = \sum_{i=-N}^{N} k_r(i) I(x-i) \tag{3}$$

$$k_r * I(x,y) = \sum_{j=-N}^{N} \sum_{i=-N}^{N} k_r(i,j) I(x-i, y-j) \tag{4}$$

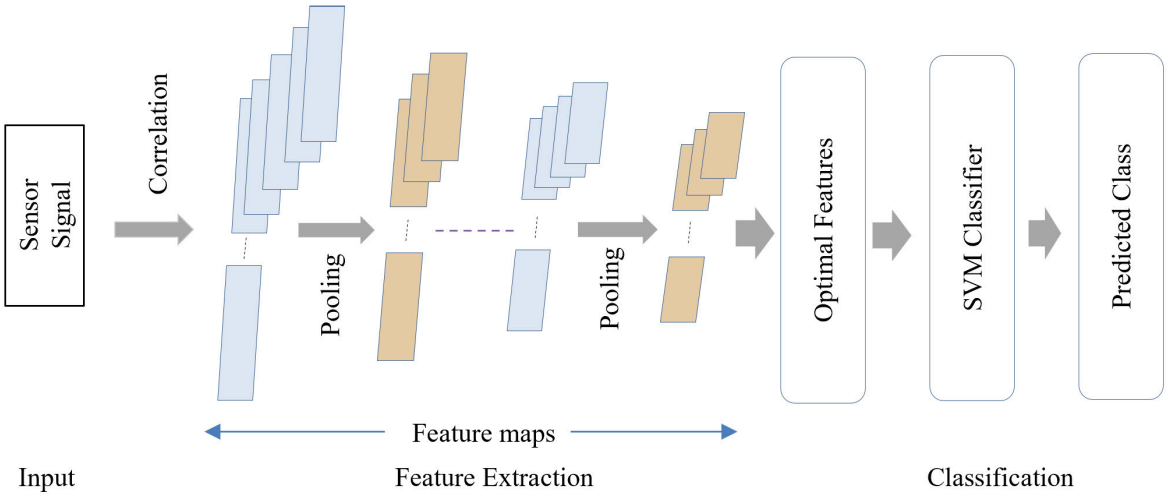

FIGURE 1. Architecture of the correlational neural network model. The network has layers of correlation and sub-sampling, followed by a classification layer.

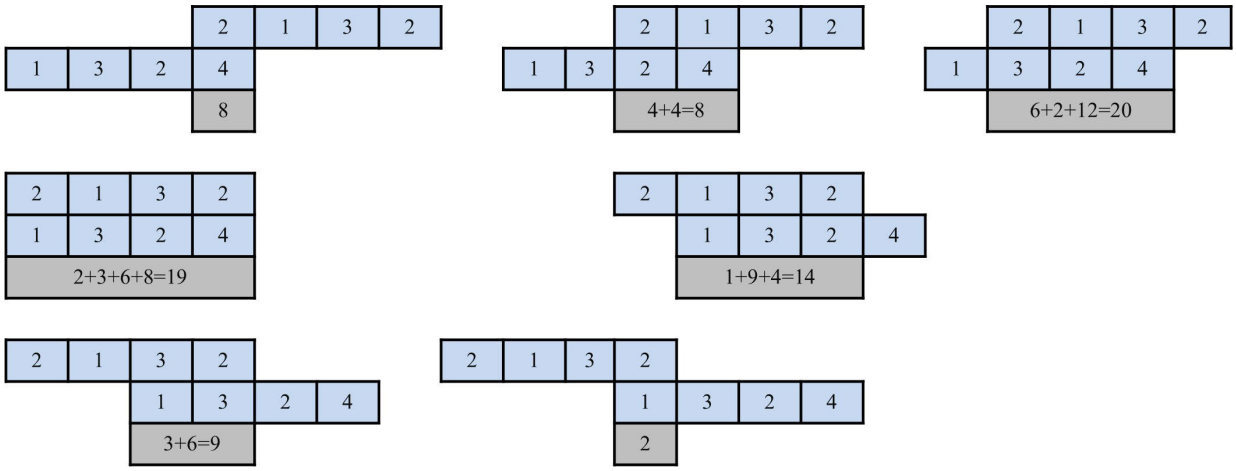

FIGURE 2. Method of finding the correlation between two signals x[n] = [1], [2], [2], [3] and k[n] = [1], [2], [3], [4].

In a typical convolution procedure, the kernel is flipped prior to convolution between the applied input signal and kernel. Convolution operations are essentially cross-correlation operations in deep learning networks as the kernel flipping is not done here. Kernels are important in the feature extraction process [17]. The kernel's values will be inverted upon flipping, delivering a different result. As a result, neural networks do not flip the kernels before the convolution process. The correlation and convolution techniques are the same when applied to deep learning networks. The correlation network presented in this paper, however, represents a novel strategy that differs from the methods already in use. The cross-correlation procedure is applied to draw the best feature maps in the proposed design. Additionally, we used adaptive kernels to run the network that were derived from the sensor signal itself.

A. PROPOSED CORRELATION OPERATION

The correlation method will determine whether there is a correlation between the kernel and the input signal. An input data-driven kernel can thoroughly analyse the signal's behaviour because the similarity between the signals is measured here. Therefore, we used adaptive kernels to carry out the correlation process. The proposed correlation operation is illustrated with an example in Fig. 2. In this example, the kernel k[n] = [1], [2], [3], [4] and the input signal x[n] = [1], [2], [2], [3] is correlated with each other. The dimensions of both of these signals are 1×4. During the correlation process, the kernel is moved over the input signal, and the overlapping values are multiplied. The values of the correlated signal are then calculated by adding the multiplied values. Each time, the kernel is moved to one sample to the right. The correlated signal is obtained as y[n] = [2], [8], [8], [9], [14], [19], [20]. The provided example demonstrates that the correlation will reach its maximum value when the input signal most closely resembles the values of the kernel.

B. ADAPTIVE KERNELS FOR CORRELATION

In this approach, the correlation between the input signal and the kernel is used to find similarities between the signals. So, choosing the best kernel for the correlation network

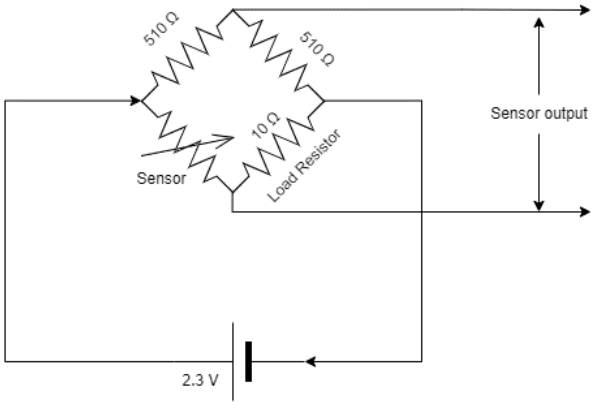

FIGURE 3. Detection circuit of the TGS1820 sensor.

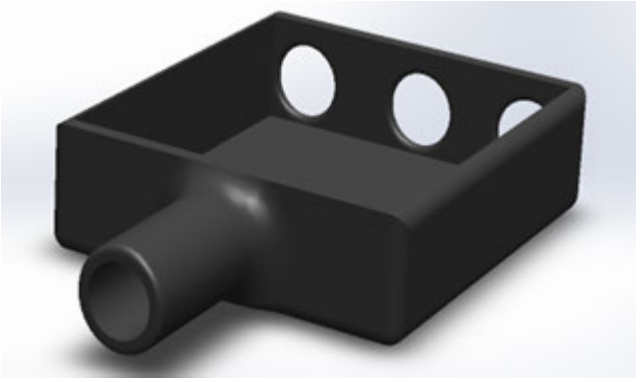

FIGURE 4. Graphical representation of the test chamber. At the front of the chamber is a mouthpiece for blowing air. The three sensors are positioned at the test chamber's back end.

is important. Depending on the correlation kernel utilised, we can derive feature maps from the signal. The choice of kernel type and size is not subject to any clear rules or restrictions. The trial-and-error approach is the ideal way to choose a kernel since it allows us to assess the network using different kernels and choose the one that yields the most useful results. Generally, a predetermined kernel like the gaussian kernel is employed in typical CNN models [18]. It will be appropriate if we select a kernel that is comparable to the input signal because the correlation gauges the similarity that exists between the signals. We, therefore, employed new kernels for the proposed neural network that were constructed and trained from the sensor data itself. Since the kernels are created using sensor data, they can easily adapt to the input signal and can analyse the behaviour of the input signal in greater detail. The specifications of the adaptive kernel are described in section III-B, along with the realisation of the proposed learning network.

III. SYSTEM DESIGN AND TESTING

A. DESCRIPTION OF THE SENSORY UNIT

Several studies have shown the use of MOS sensors in breath-based sensing. The best sensors for breath analysis are MOS sensors because of their small size, ease of use, low cost and minimal maintenance needs [19]. In this work, a new detection module based on a breath acetone gas sensor is developed. The acetone concentration is detected using an array of sensors. In the detection circuit, we used a TGS 1820 gas sensor with high acetone gas sensitivity [20]. A sintered metal oxide semiconductor material bead with a metal coil makes up the sensing element of the TGS 1820. The electrical conductivity generated by gas adsorption on the MOS material surface between the two ends of the metal coil can be measured using the change in resistance of the MOS material and the metal coil. These variations are measured and assessed using the analysis software, and the acetone concentrations can be predicted.

The detection circuit of the TGS1820 acetone sensor is depicted in Fig. 3. The circuit voltage is applied between the sensor's two ends and the load resistor, which is connected in series with the network. A circuit voltage of 2.3V is applied, and a load resistor of 10Ω is connected to the circuit, to maintain the sensing element at the ideal temperature that is suitable for acetone gas detection. A Wheatstone bridge comprised of the sensor, a load resistor, and two resistor pairs is used to measure the sensor output. The acetone sensor provides the voltage and resistance readings. It is important to track the pressure inside the chamber as improper blowing into the test chamber's mouthpiece can impact the acetone readings. A BMP180 sensor is linked to the sensor array to measure the pressure value inside the chamber [21]. A DHT11 sensor is used to measure the humidity and temperature [22]. For carrying out the testing process, we designed a test chamber. Fig. 4 displays the graphic representation of the designed test chamber. The chamber has a mouthpiece at its front for blowing the air. The three sensors are placed at the back end of the test chamber.

For the testing phase, 82 healthy individuals and 70 type 2 diabetic patients under different age groups were selected. The required procedures were followed prior to the testing process, and the study was conducted in compliance with the Declaration of Helsinki. Information about the participant groups is given in Table 2. Before the analysis, oral health guidelines were provided to all of the participants. To get the fasting glucose level, participants were instructed to fast for eight to ten hours before the test. The procedures were carried out at the District Community Medical Center under the direction of medical professionals. The volunteers were instructed to hold their breath before blowing into the mouthpiece of the test chamber. A total of 100 seconds of the sensor output are captured, with recordings made every 0.1 seconds. Therefore, the dimension of the sensor output signal will be 1×1000. The proposed deep-learning model is used directly to analyse and predict the normalized sensor signal.

The signal is normalized using the following function:

$$F'(i) = \frac{f(i) - \frac{1}{z}\sum_{n=1}^{z} f(n)}{\sqrt{\frac{1}{z}\sum_{n=1}^{z}(f(n) - \frac{1}{z}\sum_{n=1}^{z} f(n))^2}} \quad (5)$$

TABLE 2. Demographic details of the participants.

Class	Total participants	Male/ Female	Average age (Years)	Average blood glucose value (mg/dL)
Diabetic class	70	42/28	47	135.16
Healthy class	82	44/38	44	88.02

TABLE 3. Dimensions of the derived kernels for the correlation process.

Stages	Kernel dimension
1	1×1000
2	1×399
3	1×159
4	1×63
5	1×25

where z is the number of data points in the signal and f(n) is the signal sampled to 1000 points.

B. DEEP LEARNING MODULE

An advanced deep-learning CORNN model is employed for analysing the sensor output. For extracting the best features, we used the correlation operation rather than the convolution operation. We used the cross-correlation approach to obtain the ideal features for classifying the samples. Also, we have used adaptive kernels rather than predetermined kernels, which are produced from the sensor pattern itself. The correlation approach will ascertain whether there is a correlation between the input signal and the kernel [23]. A kernel trained from the input data may analyse the signal more successfully because this verifies the similarity between the signals. The size of the input signal at each phase determines the kernel size. Since the kernels are created from sensor data, they can easily adapt to the input signal and can analyze the behaviour of the input signal in greater depth.

Five correlation and pooling levels are employed to carry out the proposed correlation framework. In deep learning network design, as we already mentioned, a predetermined kernel is typically employed. So, we first used a general-purpose gaussian kernel to test our network [18]. Next, we have swapped out this kernel for the proposed adaptive kernels. As a result of the proposed kernel's higher correlation with the input signal, we achieved better results with our adaptive kernels. This shows that, in terms of correlation operation, the proposed adaptive kernel performs better than the gaussian kernel.

The kernel for the first phase should be 1×1000 in size because the sensor output signal is 1×1000 in length. To achieve this, the sensor values for each of the 82 healthy cases were averaged, and the respective signal is provided as the kernel for the first correlation layer. After that, the kernel is shifted over the input signal with a stride value of 1. The total of the products of the overlapping values is calculated concurrently. The size of the signal will therefore be 1×1999 following the initial correlation process. The max-pooling function is applied to the correlated signal because the size of the correlated signal will be large [24]. The pooling process will cut down the number of parameters, which will drastically decrease the dimension of the signal without losing the details required for prediction. By adopting the sliding window technique, pooling is done by splitting the signal into several segments while maintaining a segment size of five [25]. 399 subsections will be produced following segmentation. Max-pooling keeps the highest value from each slice of pooling. The size of the feature map created after the first stage will therefore be 1×399 in size.

The input signal of the second correlation layer will have a dimension of 1×399, so we must build a kernel with this same dimension. As a result, the kernel for this layer is derived by correlating the kernel from the first stage with itself. To ensure that the features of the kernel and correlated output are the same, the kernel is correlated. The first correlated signal's dimension will be equal to that of the correlated kernel signal. By setting the segment size at five, the output signal obtained after correlation is divided into numerous segments. The maximum value is then taken out of each pooling zone using the max-pooling approach to obtain the kernel function for the second layer. Therefore, the kernel size and the dimension of the input signal will become 1×399. The second correlated signal is then generated by performing a correlation between these two signals. The input data will be converted into a set of values with a dimension of 1×797 after the correlation operation. The signal obtained is subjected to the pooling function to minimize the feature set's dimension. As a result, the size of the feature map produced after the second layer will be 1×159.

The second kernel acts as the basis for the third stage kernel. The third stage's input will be the second layer's output. The kernel used for the second stage is correlated with itself to create the third kernel. The windowing approach is then used to split the output signal into segments. Following segmentation, max pooling is used to get the highest value from each region. To create the third kernel for the correlation, the pooling function will choose 159 samples. Consequently, the third kernel will have the dimension 1×159. This process is repeated to derive the kernel for the next two phases. As a result, 1×63 and 1×25 dimensional adaptive kernels are obtained for the next two stages. The dimensions of adaptive kernels derived for the five stages are shown in Table 3.

The result of the third correlated signal will have a dimension of 1×317. After using the third max-pooling algorithm, this correlated signal is reduced to 1×63 samples. The input signal will have a dimension of 1×125 after the fourth correlation procedure. This will drop to 25 samples after the pooling procedure is applied. As a result, the last stage's input signal will have a dimension of 1×25. The

output signal will be generated with a dimension of 1×49 after applying the kernel with the same dimension. The final pooling process reduces the size of the correlated signal to 1×9. The features map, which is obtained from the reduced signal after the last pooling layer, is used to classify the data.

The best features are obtained after five levels of correlation and pooling procedures. Lastly, the retrieved features are assigned to the classification layer for performing the classification to predict the class. The features obtained during the feature extraction process are transferred to the network's classification layer, which is the last layer. A Multilayer Perceptron (MLP) with an activation function serves as the fully connected classification layer in a CNN [26]. Based on the input feature sets, weights and activation function, the MLP network predicts the output. To improve prediction accuracy, we combined the proposed correlation network with a Support Vector Machine (SVM) classifier to create a hybrid model. A kernel based on the Radial Basis Function (RBF) is used to implement the classifier [27]. The classifier's parameter values are chosen at random. SVM will classify the data set by designating certain datasets as positive and others as negative sets. Based on the provided data sets, the support vectors are established, and the viability of the hyper-plane is determined.

The SVM's classification function is described as follows:

$$f_x = I_x\omega - b \tag{6}$$

where b stands for the bias value and I and ω are the input and weight vectors, respectively.

The criteria used for classification are as follows:

$$I_x\omega - b > 0, \quad h_x = 1 \tag{7}$$

$$I_x\omega - b < 0, \quad h_x = -1 \tag{8}$$

The defined hypothesis, h_x, designates a case that is either normal or abnormal. The classification criterion is generalized as follows:

$$h_i(I_i\omega_i - b) \geq 0 \tag{9}$$

The following equation describes the classification margin of SVM:

$$C_{mar} = \frac{1}{\| \omega \|} \tag{10}$$

The SVM classifier's training issue is regarded as an optimization problem [28]. By minimising $\|\omega\|$, the hyperplane is established for the SVM classifier's optimization. The margin of separation will increase if $\|\omega\|$ is valued less.

$$f_x(w) = \frac{1}{2}\| \omega \|^2 \tag{11}$$

For the objective of identifying the solution, the Lagrangian function must be represented in the dual form.

$$L(\omega, b, \alpha) = \frac{1}{2}\| \omega \|^2 - \sum_{i=1}^{N} \alpha_i h_i I_i \omega + b \sum_{i=1}^{N} \alpha_i h_i + \sum_{i=1}^{N} \alpha_i \tag{12}$$

where α is the Lagrange multiplier.

The SVM classifier selects the ideal hyper-plane to maximise the boundary of the division line that divides the identified support vectors. The best hyperplane is then determined by computing the ω and b.

$$\omega = \sum_{i=1}^{n} \alpha_i h_i I_i \tag{13}$$

$$b = \frac{1}{v_s} \sum_{i=1}^{v_s} (h_i - I\omega) \tag{14}$$

where v_s represents the number of support vectors.

The RBF kernel function is used to determine the degree of resemblance or proximity between two points of interest, X1 and X2. This kernel has the following mathematical representation:

$$k_{RBF}(X_1, X_2) = e^{\frac{-\|X_1 - X_2\|^2}{2\sigma^2}} \tag{15}$$

where the Euclidean distance between two points is represented by $\| X_1 - X_2 \|$ and σ is the hyperparameter.

IV. RESULTS AND DISCUSSION

The objective of this study is to build an automated diagnosis system for detecting diabetes from exhaled breath. Machine learning and deep learning algorithms are employed in this work to make automated predictions of the tested samples. The presence of the targeted compound acetone will cause the sensing material of the sensor to react, and the electrical characteristics of the sensor will vary accordingly. The sensor out signal is directly given as the input to the machine learning and deep learning models for automatically analyzing the sensor response and making predictions. The proposed learning model is programmed and trained in the Matlab R2022b tool. The normalised sensor data is used to train and test the proposed CORNN model and to make automated predictions. Various traditional learning networks are implemented and tested along with this proposed model to analyse and compare the outcomes [29].

A. PERFORMANCE ANALYSIS OF THE SENSING MODULE

The sensory unit we employed here is based on a new methodology; therefore, it is necessary to assess the capability of the sensor to detect diabetes using a recognised diabetes detection method. The sensor used here has a 1 to 10 ppm detection range. The sensor was first exposed to a range of acetone gas concentrations to evaluate its response. The recorded voltage readings for the various acetone concentration levels are shown in Fig. 5. The standard medical procedure for

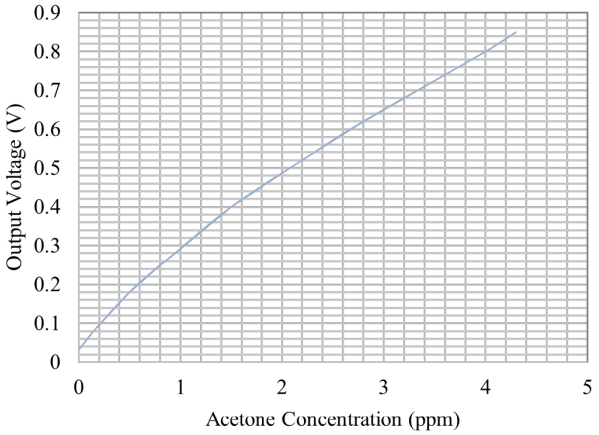

FIGURE 5. Sensor response for variations in acetone gas concentration.

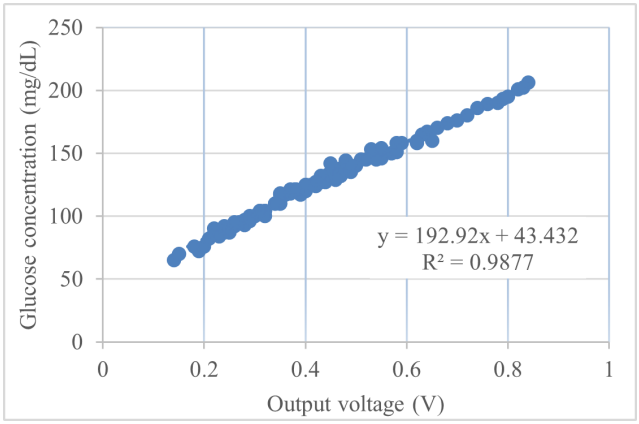

FIGURE 6. Plot of statistical analysis. The derived regression line equation is y = 192.92x + 43.432 with a R^2 value of 0.9877.

detecting diabetes is a blood-based screening procedure. The blood sample is placed on a glucose testing strip with glucose-oxidase, which combines with the blood glucose to produce the desired result. The glucose level of the blood sample is then determined using a glucometer. A fasting blood sugar level of less than 100 mg/dL is considered normal. Fasting blood sugar readings of 100 to 125 mg/dL are considered prediabetic. When the blood glucose level is 126 mg/dL more, diabetes is considered to be present [30].

To support and corroborate our findings, we measured the blood glucose levels of each participant using the conventional method. The data are analysed to determine the effectiveness of the sensing module using Pearson's correlation and a regression model [31]. Statistics are used to assess the degree of correlation between the readings obtained from the proposed sensing model and blood-based screening. We observed an extremely strong correlation between the voltage values obtained from the sensor and the blood glucose values, with an r value of 0.9938. The scatter plot for this analysis is shown in Fig. 6. For this assessment, the regression line equation obtained is $y = 192.92x + 43.432$. The regression analysis statistical indicator (R^2) is calculated to be 0.9877.

The proposed system is not making predictions based on blood glucose values. The sensor response signal is analyzed with the help of machine learning and deep learning algorithm to classify the samples automatically. The correlation and regression analysis is only done to demonstrate that diabetes can be identified by monitoring the amount of acetone gas in the exhaled breath sample because there is a strong positive correlation between the levels of acetone in exhaled breath and glucose level in the blood sample. This implies that the acetone concentration in the exhaled breath increases with an increase in blood glucose levels.

Voltage, resistance, humidity, temperature and pressure values are measured in the analysis. To account for the effects of operational temperature and humidity, we have included a temperature and humidity sensor in the sensor array. Measuring the pressure of breath is important as improper blowing can impact the acetone readings. According to the test results, voltage and resistance are the key factors in the detecting process, with the other factors having little impact on the data. A test sample's voltage, resistance, pressure, humidity and temperature variations over time are shown in Fig. 7. It is apparent from Fig. 7 that the voltage value of the sensor increases along with rising glucose concentrations. Temperature and humidity had no discernible effect on our test results because testing is conducted in a controlled environment under normal working conditions. Temperature and humidity effects can be offset by adjusting the sensor signal appropriately. In a few instances, we observed that when the pressure values were low, the voltage and resistance values slightly decreased. This occurred as a result of the participant's improper blow into the detecting chamber. Accordingly, when taking the acetone measurement, it is important to consider the pressure of exhaled breath into account.

B. PERFORMANCE ANALYSIS OF THE CLASSIFICATION MODELS

We have considered the recent works related to non-invasive diabetic detection in this work. There are a few studies where the authors used a sample of exhaled breath to identify diabetes. However, these works use different sensing modules. In this work, we have designed and implemented a new sensing approach for the detection process. Because of this, a direct comparison with the results of the data classification methods discussed in other research publications will not be appropriate. However, in order to compare the results of the proposed neural network model, we implemented the conventional data classification algorithms and tested them with the proposed sensing module to detect diabetes. Conventional and classical data classification algorithms are implemented to evaluate the effectiveness of the proposed network. Along with the proposed CORNN model, we have also implemented the traditional SVM with Singular Value Decomposition (SVD), the K-Nearest Neighbours (KNN) classification algorithm with Principal Component Analysis (PCA) as the

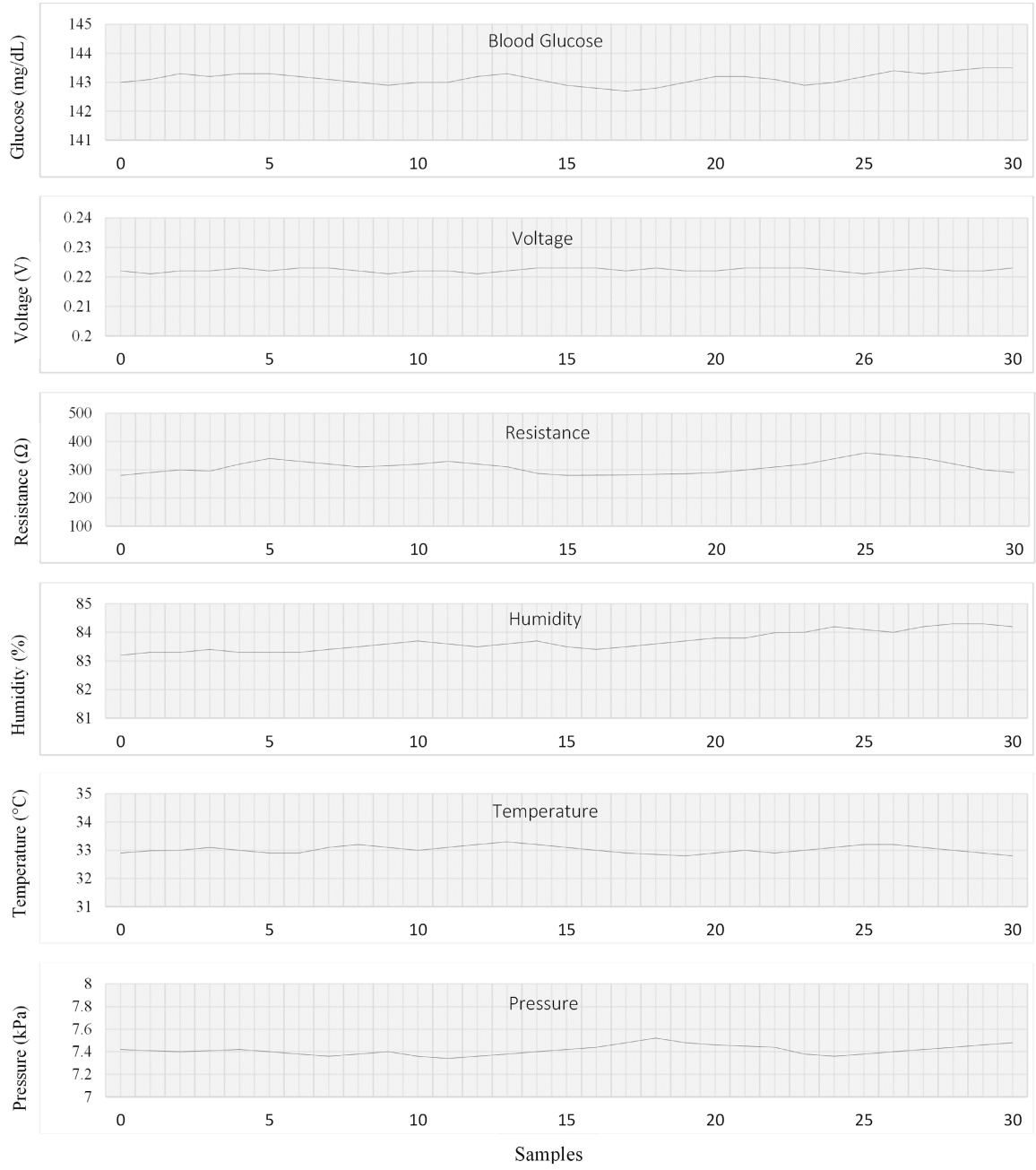

FIGURE 7. Variations in a test patient's blood glucose, sensor output voltage, resistance, pressure, humidity and temperature readings over a time interval, with recordings made every 0.1 seconds.

feature extractor, the Shallow CNN, the Recurrent Neural Network (RNN) model, the CNN-Random Forest (RF) combination network, the CNN-MLP model and the CNN-SVM combination network [32], [33], [34], [35], [36]. Both, SVM and MLP classifiers are used to classify the samples obtained after the correlation process. The performance of each of these learning models is analysed in this section.

To evaluate the performance of the CORNN hybrid model, the important performance parameters are computed. From the components of the generated confusion matrix, all parameter values are obtained. The proposed correlation network's performance is contrasted with that of classical techniques in Table 4. In addition to accuracy, we have evaluated the sensitivity, specificity, precision, F1 score, Matthews Correlation Coefficient (MCC), False Discovery Rate (FDR), False Omission Rate (FOR) and error rates of the classification networks [37]. While KNN is a classifier like SVM, SVD and PCA algorithms are feature extraction methods. SVD-SVM, PCA-SVM and PCA-KNN are examples of conventional machine learning approaches. These models employ two separate feature extraction and classification techniques for analysis. The accuracy of the predictions made by the SVD-SVM, PCA-SVM and PCA-KNN networks are 86.84%, 88.16% and 82.89%, respectively.

TABLE 4. Comparison of performance measures of the proposed CORNN networks and other classical data classification techniques.

Classification Models	Accuracy (%)	Sensitivity (%)	Specificity (%)	Precision	FDR	FOR	F1 score	MCC	Error rate
SVD with SVM classifier	86.84	83.78	89.74	0.885	0.114	0.146	0.861	0.737	0.131
PCA with KNN classifier	82.89	80.56	85.01	0.828	0.171	0.17	0.817	0.657	0.171
PCA with SVM classifier	88.16	86.11	90.02	0.886	0.114	0.122	0.873	0.762	0.118
RNN Model	83.55	81.69	85.18	0.828	0.171	0.158	0.823	0.669	0.164
ShallowCNN Model	91.45	91.3	91.57	0.9	0.1	0.073	0.906	0.828	0.085
CNN with RF classifier	93.42	91.67	95.01	0.943	0.057	0.073	0.929	0.868	0.065
CNN with MLP classifier	95.39	95.65	95.18	0.943	0.057	0.036	0.949	0.907	0.046
CNN with SVM classifier	96.05	95.71	96.34	0.957	0.043	0.036	0.957	0.92	0.039
Proposed CORNN with MLP classifier	97.37	97.14	97.56	0.971	0.028	0.024	0.971	0.947	0.026
Proposed CORNN with SVM classifier	98.02	98.55	97.59	0.971	0.028	0.012	0.978	0.96	0.02

Deep learning networks like CNN automatically extract features from input signals. As a result, CNN-based networks could provide greater efficiency than conventional machine learning models. CNN model that has only one hidden layer is called shallow CNN [38]. Also, we have deployed a deep-learning CNN with five layers. The classification accuracy for the single-layer CNN is 91.45%. With five layers, CNN-SVM model correctly classified the test samples with 96.05% accuracy. CNN combined with RF network classified the test samples with an accuracy of 93.42%. When compared to the other models taken into consideration for this evaluation, the proposed CORNN model attained the highest accuracy. The accuracy of the CORNN model with MLP classifier for predicting diabetes is obtained as 97.37%. After adding the SVM classifier to the CORNN model, the prediction accuracy of the model improved. The performance of the CORNN hybrid model with different kernels is also examined. Better performance of classification was achieved with the RBF kernel. The test samples were classified with 98.02% accuracy by the CORNN-SVM hybrid network using an RBF kernel. Compared to all other techniques, this network's error rate is relatively low at 0.02.

In typical machine learning networks, decreasing computing time is important since training and testing take longer when the data's dimensions are huge. Table 5 compares the execution timings of the various data classification networks taken into account in this study. Traditional machine learning techniques (SVD-SVM, PCA-SVM, and PCA-KNN) take longer to execute since they employ separate algorithms for feature extraction and classification. The average feature extraction time for the proposed deep learning CORNN model is 1.163 seconds. The MLP classifier predicts the class in 1.789 seconds. The total computing time for this network is 2.952s. The CORNN-SVM hybrid model has taken only 2.592s for computation. The significant reduction in processing time that deep learning networks offer has led to their increased popularity.

TABLE 5. Execution time of the different learning networks.

Models	Feature extraction time (seconds)	Classification time (seconds)	Total computational time (seconds)
SVD-SVM	1.942	1.879	3.821
PCA-KNN	1.942	2.26	4.202
PCA-SVM	1.921	1.842	3.763
Shallow CNN	0.545	2.332	2.877
CNN-RF	0.946	1.942	2.888
CNN-MLP	0.978	1.798	2.776
CNN-SVM	0.949	1.467	2.416
CORNN-MLP	1.163	1.789	2.952
CORNN-SVM	1.124	1.468	2.592

TABLE 6. Validation results with number of samples misclassified.

Models	Patient Class	Healthy Class	Misclassified Samples
CNN-MLP	65	87	7
CNN-SVM	65	87	6
CORNN-MLP	67	85	4
CORNN-SVM	68	84	3

C. VALIDATION OF RESULTS

Clinical validation is done to validate the test outcomes. We conducted the validation test with the assistance of medical professionals, and the results were approved by the physician. The validation findings are shown in Table 6 along with the number of samples that were misidentified. The clinical evaluation's findings have nearly mirrored those of our test results. Out of the 152 samples that were analysed, the proposed deep learning model classified 68 samples as diabetes and 84 samples as healthy. This model misclassified only three samples. The proposed model accurately classified all of the healthy samples in the healthy group. To validate the relevance of the change in the model's classification accuracy, we used a t-test. We had a p-value of under 0.05 for the suggested model. This demonstrates that the outcome was not a random occurrence and that it is statistically significant.

V. CONCLUSION

In this paper, a novel sensing module and an efficient deep-learning neural network model are proposed for the non-invasive and automated detection of diabetes. To effectively manage diabetes and to reduce the health issues associated with diabetes, early detection of the disease is important. This study describes a breath-based diagnosis method that offers several advantages over conventional methods. The outcomes of the proposed system are compared with the traditional blood-based diagnosis method. We observed a strong positive correlation between the two results with r and R^2 values of 0.9938 and 0.9877, respectively. The statistical analysis suggests that the proposed sensing approach has the potential to be used as a non-invasive technique for detecting diabetes. The CORNN hybrid model performs better in terms of data classification and prediction accuracy than other traditional approaches. The proposed medical system predicted diabetes with an accuracy of 98.02%. On the basis of our research, we draw the conclusion that the proposed method is effective and can be used in clinical practice to non-invasively detect diabetes.

REFERENCES

[1] M. K. Hasan, M. A. Alam, D. Das, E. Hossain, and M. Hasan, "Diabetes prediction using ensembling of different machine learning classifiers," *IEEE Access*, vol. 8, pp. 76516–76531, 2020.

[2] K. Ogurtsova, L. Guariguata, N. C. Barengo, P. L.-D. Ruiz, J. W. Sacre, S. Karuranga, H. Sun, E. J. Boyko, and D. J. Magliano, "IDF diabetes atlas: Global estimates of undiagnosed diabetes in adults for 2021," *Diabetes Res. Clin. Pract.*, vol. 183, Jan. 2022, Art. no. 109118.

[3] G. Faura, G. Boix-Lemonche, A. K. Holmeide, R. Verkauskiene, V. Volke, J. Sokolovska, and G. Petrovski, "Colorimetric and electrochemical screening for early detection of diabetes mellitus and diabetic retinopathy—Application of sensor arrays and machine learning," *Sensors*, vol. 22, no. 3, p. 718, Jan. 2022.

[4] A. T. Güntner, I. C. Weber, S. Schon, S. E. Pratsinis, and P. A. Gerber, "Monitoring rapid metabolic changes in health and type-1 diabetes with breath acetone sensors," *Sens. Actuators B, Chem.*, vol. 367, Sep. 2022, Art. no. 132182.

[5] S. Lekha and M. Suchetha, "Real-time non-invasive detection and classification of diabetes using modified convolution neural network," *IEEE J. Biomed. Health Informat.*, vol. 22, no. 5, pp. 1630–1636, Sep. 2018.

[6] A. Paleczek and A. Rydosz, "Review of the algorithms used in exhaled breath analysis for the detection of diabetes," *J. Breath Res.*, vol. 16, no. 2, Apr. 2022, Art. no. 026003.

[7] R. Selvaraj, N. J. Vasa, S. M. S. Nagendra, and B. Mizaikoff, "Advances in mid-infrared spectroscopy-based sensing techniques for exhaled breath diagnostics," *Molecules*, vol. 25, no. 9, p. 2227, May 2020.

[8] R. E. Melo, T. A. Popov, and D. Solé, "Exhaled breath temperature, a new biomarker in asthma control: A pilot study," *Jornal Brasileiro Pneumologia*, vol. 36, pp. 693–699, Jan. 2010.

[9] C. Popa, D. C. A. Dutu, R. Cernat, C. Matei, A. M. Bratu, S. Banita, and D. C. Dumitras, "Ethylene and ammonia traces measurements from the patients' breath with renal failure via LPAS method," *Appl. Phys. B, Lasers Opt.*, vol. 105, no. 3, pp. 669–674, Nov. 2011.

[10] S. Mendis, P. A. Sobotka, and D. E. Euler, "Expired hydrocarbons in patients with acute myocardial infarction," *Free Radical Res.*, vol. 23, no. 2, pp. 117–122, Jan. 1995.

[11] S. M. Sivertsen, A. Bjørneklett, H. P. Gullestad, and K. Nygaard, "Breath methane and colorectal cancer," *Scandin. J. Gastroenterol.*, vol. 27, no. 1, pp. 25–28, Jan. 1992.

[12] D. Smith, P. Španěl, F. J. Gilchrist, and W. Lenney, "Hydrogen cyanide, a volatile biomarker of *Pseudomonas aeruginosa* infection," *J. Breath Res.*, vol. 7, no. 4, Nov. 2013, Art. no. 044001.

[13] Z. Wang and C. Wang, "Is breath acetone a biomarker of diabetes? A historical review on breath acetone measurements," *J. Breath Res.*, vol. 7, no. 3, Aug. 2013, Art. no. 037109.

[14] N. Kumar, N. N. Das, D. Gupta, K. Gupta, and J. Bindra, "Efficient automated disease diagnosis using machine learning models," *J. Healthcare Eng.*, vol. 2021, Mar. 2021, Art. no. 9983652.

[15] B. Navaneeth and M. Suchetha, "PSO optimized 1-D CNN-SVM architecture for real-time detection and classification applications," *Comput. Biol. Med.*, vol. 108, pp. 85–92, May 2019.

[16] Q. Feng and B. Li, "Convolution and correlation theorems for the two-dimensional linear canonical transform and its applications," *IET Signal Process.*, vol. 10, no. 2, pp. 125–132, Apr. 2016.

[17] M. A. Mahmoudi, A. Chetouani, F. Boufera, and H. Tabia, "Kernel-based convolution expansion for facial expression recognition," *Pattern Recognit. Lett.*, vol. 160, pp. 128–134, Jan. 2022.

[18] X. Wang, S. Yin, K. Sun, H. Li, J. Liu, and S. Karim, "GKFC-CNN: Modified Gaussian kernel fuzzy C-means and convolutional neural network for apple segmentation and recognition," *J. Appl. Sci. Eng.*, vol. 23, no. 3, pp. 555–561, 2020.

[19] Y. Li, M. Zhang, and H. Zhang, "Acetone sensors for non-invasive diagnosis of diabetes based on metal–oxide–semiconductor materials," *Chin. Phys. B*, vol. 29, no. 9, Sep. 2020, Art. no. 090702.

[20] A. Paleczek, D. Grochala, and A. Rydosz, "Artificial breath classification using XGBoost algorithm for diabetes detection," *Sensors*, vol. 21, no. 12, p. 4187, 2021.

[21] A. Á. Moya and A. Merino, "Building a digital barometer with Arduino to study forces due to atmospheric pressure and weather maps at schools," *Phys. Educ.*, vol. 57, no. 4, Jul. 2022, Art. no. 045018.

[22] B. Vallabh, A. Khan, D. Nandan, and M. Choubisa, "Data acquisition technique for temperature measurement through DHT11 sensor," in *Proc. 2nd Int. Conf. Smart Energy Commun.* Singapore: Springer, 2021, pp. 547–555.

[23] N. Bhaskar, M. Suchetha, and N. Y. Philip, "Time series classification-based correlational neural network with bidirectional LSTM for automated detection of kidney disease," *IEEE Sensors J.*, vol. 21, no. 4, pp. 4811–4818, Feb. 2021.

[24] B. Navaneeth and M. Suchetha, "A dynamic pooling based convolutional neural network approach to detect chronic kidney disease," *Biomed. Signal Process. Control*, vol. 62, Sep. 2020, Art. no. 102068.

[25] M. Sun, Z. Song, X. Jiang, J. Pan, and Y. Pang, "Learning pooling for convolutional neural network," *Neurocomputing*, vol. 224, pp. 96–104, Feb. 2017.
[26] Y. Wei, J. Jang-Jaccard, F. Sabrina, A. Singh, W. Xu, and S. Camtepe, "AE-MLP: A hybrid deep learning approach for DDoS detection and classification," *IEEE Access*, vol. 9, pp. 146810–146821, 2021.
[27] M. Amirian and F. Schwenker, "Radial basis function networks for convolutional neural networks to learn similarity distance metric and improve interpretability," *IEEE Access*, vol. 8, pp. 123087–123097, 2020.
[28] J. Cervantes, F. Garcia-Lamont, L. Rodríguez-Mazahua, and A. Lopez, "A comprehensive survey on support vector machine classification: Applications, challenges and trends," *Neurocomputing*, vol. 408, pp. 189–215, Sep. 2020.
[29] N. Bhaskar and M. Suchetha, "A computationally efficient correlational neural network for automated prediction of chronic kidney disease," *IRBM*, vol. 42, no. 4, pp. 268–276, Aug. 2021.
[30] O. P. Adams, "The impact of brief high-intensity exercise on blood glucose levels," *Diabetes, Metabolic Syndrome Obesity, Targets Therapy*, vol. 10, pp. 113–122, Feb. 2013.
[31] J. Gravier, V. Vignal, S. Bissey-Breton, and J. Farre, "The use of linear regression methods and Pearson's correlation matrix to identify mechanical–physical–chemical parameters controlling the micro-electrochemical behaviour of machined copper," *Corrosion Sci.*, vol. 50, no. 10, pp. 2885–2894, Oct. 2008.
[32] L. Zhu, S. Zhang, H. Zhao, S. Chen, D. Wei, and X. Lu, "Classification of UAV-to-ground vehicles based on micro-Doppler signatures using singular value decomposition and deep convolutional neural networks," *IEEE Access*, vol. 7, pp. 22133–22143, 2019.
[33] D. Zhang, J. Yang, F. Li, S. Han, L. Qin, and Q. Li, "Landslide risk prediction model using an attention-based temporal convolutional network connected to a recurrent neural network," *IEEE Access*, vol. 10, pp. 37635–37645, 2022.
[34] M. Belgiu and L. Drăguţ, "Random forest in remote sensing: A review of applications and future directions," *ISPRS J. Photogramm. Remote Sens.*, vol. 114, pp. 24–31, Apr. 2016.
[35] J. Kim, J. Choi, Y. Park, C. K. Leung, and A. Nasridinov, "KNN-SC: Novel spectral clustering algorithm using k-Nearest neighbors," *IEEE Access*, vol. 9, pp. 152616–152627, 2021.
[36] I. T. Jolliffe and J. Cadima, "Principal component analysis: A review and recent developments," *Phil. Trans. Roy. Soc. A, Math., Phys. Eng. Sci.*, vol. 374, no. 2065, Apr. 2016, Art. no. 20150202.
[37] D. Chicco and G. Jurman, "The advantages of the Matthews correlation coefficient (MCC) over F1 score and accuracy in binary classification evaluation," *BMC Genomics*, vol. 21, no. 1, pp. 1–13, Dec. 2020.
[38] F. Gao, T. Wu, J. Li, B. Zheng, L. Ruan, D. Shang, and B. Patel, "SD-CNN: A shallow-deep CNN for improved breast cancer diagnosis," *Computerized Med. Imag. Graph.*, vol. 70, pp. 53–62, Dec. 2018.

NAVANEETH BHASKAR received the Engineering degree in electronics and communication engineering and the M.Tech. degree in digital electronics and communication systems from Visvesvaraya Technological University, and the Ph.D. degree in machine learning from VIT University, India. He is currently an Associate Professor with the Department of Computer Science and Engineering (Data Science), Sahyadri College of Engineering and Management, India. He has published many papers in national and international conferences and reputed journals. His research interests include artificial intelligence, machine learning, data analytics, the IoT, and Signal processing. He is a Life Member of the Data Science Association and the International Association of Engineers.

VINAYAK BAIRAGI (Senior Member, IEEE) received the M.E. degree in electronics, in 2007, and the Ph.D. degree in engineering from the University of Pune, in 2013. He has teaching experience of 16 years and research experience of ten years. He has filed 12 patents and five copyrights in the technical field. He has published more than 61 articles, of which 38 articles are in international journals. His 55 articles are indexed in Scopus and 32 articles are indexed in SCI. He has received four research grants. He was invited as the Session Chair for 21 national and international conferences. He is the Chair of the IEEE Signal Processing Society Pune Chapter from 2020 to 2023.

EKKARAT BOONCHIENG (Senior Member, IEEE) received the B.S. degree in computer science from Khon Kaen University, Thailand, the M.S. degree in computer science from the University of New Haven, USA, and the Ph.D. degree in computer science from the Illinois Institute of Technology, USA, under the Thai Government Scholarship. He has been an Associate Professor with the Department of Computer Science, Faculty of Science, Chiang Mai University, Chiang Mai, Thailand. His research interests include computer graphics, image processing, data science, and biomedical engineering.

MOUSAMI V. MUNOT received the M.Tech. degree and the Ph.D. degree from the College of Engineering, Pune, Savitribai Phule Pune University, in 2007 and 2013, respectively. She has received a fellowship from the Indian National Academy of Engineering (INAE) for research work. She has 13 years of teaching experience and seven years of research experience. She has also received support from DST (ITS) to present a research paper at IET–Image Processing Conference, London, U.K. She has fetched grants worth nine lakhs from DST and SPPU-BCUD for funded research projects. She is a member of IET, ISTE, BMESI, and IoE. She is a reviewer for various reputed journals.